KTH Engineering Sciences

Bachelor Thesis in UHECR detection and the JEM-EUSO mission

Firas Beshoory
beshoory@kth.se

SA107X Degree Project in Engineering Physics, First Level
Supervisor: Christer Fuglesang

Department of Physics
School of Engineering Sciences
Royal Institute of Technology (KTH)

July 1, 2014

Abstract

The interest in high-energy astrophysics and to venture beyond the standard model has driven theoretical and experimental physicists around the world to collaborate and build the necessary instrumentation to test out all the different theories in particle physics. Energies up to 14 TeV have been thoroughly investigated so far by colliding protons in the Large Hadron Collider (LHC). Cosmic ray maps showed us the existence of even higher energies coming from outer space. What is the nature of such particles, and why do they accelerate to as much as $10^{20}eV$? The study of Ultra High-Energy Cosmic Rays (UHECR) is a new and active research area where physicists hope to find the sources of such high-energy particles and confirm already existing theories.

This thesis discusses the detections of UHECR, and more specifically the space approach. The ongoing project JEM-EUSO is planned to be launched in 2018 by the Japanese heavy liftrocket H2B, and conveyed to the International Space Station (ISS), where it is thought to gather more data than what already have been obtained all the previous years from the earth's surface.
The detection of UHECR occurs through the "atmospheric detector", where an incoming particle makes a shower of secondary particles in the atmosphere called Extensive Air Shower (EAS) upon contact. This shower of particles yields both flourenscence light and Cherenkov light. The problem at hand is to figure out the amount and distribution of the photons created, and how many of these photons actually will reach the detectors of the JEM-EUSO up on the ISS.

Contents

List of Abbreviations

CD	Cherenkov detector
CL	Cherenkov light
CMB	cosmic microwave background
CR	cosmic ray
EAS	extensive air shower
FD	fluorescence detector
FL	fluorescence light
GZK	initials of Greisen, Zatsepin, and Kuzmin
ISS	Internation Space Station
JEM-EUSO	the Japanese Experiment Module of the Extreme Universe Space Observatory
MD	muon detector
PP	pair production
SD	surface detector
UHE	ultra-high energy
UHECR	ultra-high energy cosmic rays

Chapter 1

Introduction

In this chapter a brief historical background for the concept of cosmic rays will be presented. The main objective of this thesis is to find out the amount of photons that will reach JEM-EUSO in space, however it will be covered later on in Chapter 3, once a full understanding of the extensive air shower (EAS) mechanism is acquired from Chapter 2.

1.1 Cosmic Rays

Viktor Hess measured in 1912 the electrification of air in a balloon flight to an altitude of 5300 m and noticed that the ionization rate decreased with rising altitude as it was expected though only up to $\sim 700\ m$. Above that point it started to increase, and was up to four times the rate at ground level! [1] In his own words the conclusion he arrived to was:

> The results of my observation are best explained by the assumption that a radiation of very great penetrating power enters our atmosphere from above.

which led later on to the discovery of cosmic rays (CRs). During the thirties CRs were studied and utelized by Carl D. Anderson et al. in the discovery of positron, muon, and pion particles [2]. Moreover the confirmation of Dirac's theory of antiparticles in these years led Heitler [3] and others to the first detailed explanation on the formation of CR generated showers.
Later on in 1948 heavy nuclei in the shower had been confirmed by sending cloud chambers 30 km up in the air. One year later Fermi took the first steps into solving the mystery of the origins of CRs, who proposed a theory where CR particles have more probability to accelerate than to decelerate in the presence of interstellar magnetic fields [4].

Starting in the fifties plastic scintillators were implemented in CR detectors, backed up with photomultiplier tubes (PMTs), which brought much better time resolution for coincidence measurements. It served the other main goal of exploring the properties of the primary incoming CR particles, where the output signal became proportional to the amount of charged particles entering the detector. Reconstructing these properties from the EAS structure, especially the higher end of the energy spectrum, had become the main aspect of research. Major contributions in this decade were made by Rossi in the US and Zatsepin in the USSR, where arrival direction and energy of the incoming cosmic

particle were obtained through the information of timing and signal intensity from an array of plastic scintillators. Energies up to $10^{18}eV$ were measured for the first time. However this technique was utilized in the 60s in the Volcano Ranch array [5] built by John Linsley and Livio Scarsi. In 1962 Linsley witnessed a shower produced by a primary of energy exceeding $10^{20}eV$.

In the 1960s a new technique was introduced independently by Greisen [7], Chudakov [6] and various others: the air fluorescence technique. This method for detection however was applied no sooner than the end of the seventies, when it was carried out by Mason et al.. The basic principle of this method is to detect the emitted UV fluorescence light (FL) created by the extended air showers within the atmosphere, hence allowing us to observe the entire longitudinal development of the shower. This was accomplished by structuring an array of detectors of wide angle UV tepescopes monitoring the sky during clear dark nights.

Greisen [8] and independently Zatsepin and Kuzmin predicted in 1966 that CR energies above $3 - 4 * 10^{19}eV$ should have limited propagation length in space due to their interaction with the cosmic microwave background (CMB), later known as the GZK-limit. In the same year Haverah Park started operation detecting several CRs over $10^{20}eV$ through its 20 years of operation. This experiment targeted Cherenkov light (CL) produced by secondaries (particles created in the shower) and detected in water tanks through PMTs installed on the walls of the tanks.

Based on the successful attempt made on detecting FL in 1977 a new observatory started operating in 1981 in the western Utah desert; named Fly's Eye [9], and it consisted of UV telescopes. The highest energy particle ever recorded was detected in this observatory in 1991. With its humongous energy of $3.1 * 10^{20}eV$ it became known as the "Oh-my-God Particle".
In 1993 the experiment was upgraded with larger mirrors and finer pixels for higher exposure, lower threshold energy and better event reconstruction, hence it was renamed to HiRes Fly's Eye.

The next major experiment in this field, the Akeno Giant Air Shower Array [10] (AGASA), was carried out in Japan, which started operation in 1990. Here a plastic scintillator array was arranged over about $100km^2$ consisting of 111 surface detectors (SDs) and 27 under absorbers / muon detectors (MDs), with the intention of exploring the most energetic part of the spectrum.

A disagreement arose between HiRes and AGASA over the presence of the GZK cutoff, though was later solved by merging fluorescence detectors (FDs) with Cherenkov detectors (CDs) through a systematic uncertainity on the energy scale combining the two techniques. This concept was implemented by the Piere Auger Observatory on the vast plains in western Argentina, which started operation in 2004. It is a collaboration of various institutions around the world, and currently the largest detector array covering an area of $3000km^2$ [11].

Due to the power law nature of the spectrum, better statistical results for energies around the GZK cutoff can be obtained through larger detectors. Covering larger areas than Piere Auger Observatory is somewhat unrealistic, though luckily there has been another approach dormant these past years suggested by J. Linsley in 1981, namely the space approach [12]. In other words, by detecting FL and CL from space the spatial limitation is lifted. The JEM-EUSO mission will apply this approach by mounting a telescope abroad the ISS.

1.2 Cosmic Ray Spectrum and high energy particles

The arrival of e.g. 50 keV x-ray photons from space is evidence of particles with at least that much energy, and often much more, since each photon comes from a single particle. No process exists by which, for instance, ten electrons with 5 keV each combine their energy to create a single photon of 50 keV [13]. This means that detected particles at the UHE level do in fact accelerate to such high energies.

The CR energy spectrum spans energies from 10^8 eV to over 10^{20} eV, and it is usually described metaphorically by a leg with a "knee" at around $3-4$ PeV (10^{15} eV), and an "ankle" in the order of EeV (10^{18} eV), see figure 1.1.

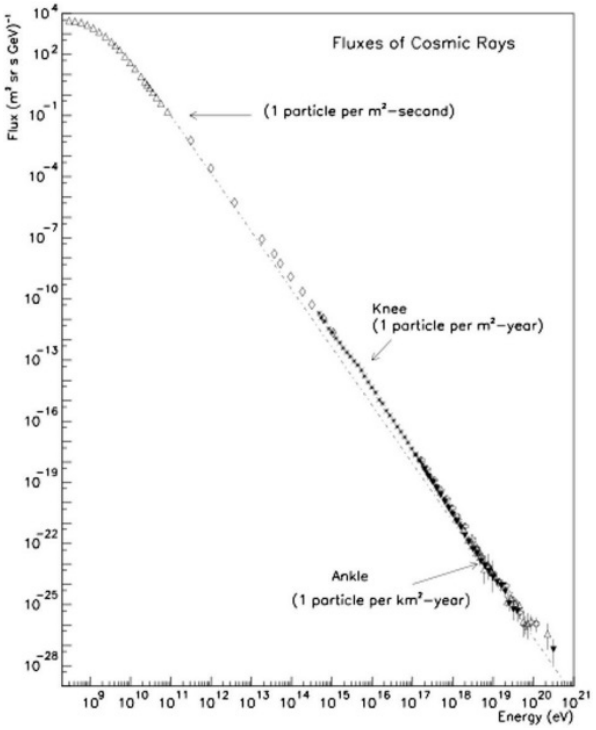

Figure 1.1: The CR energy spectrum as published by Swordy in 2001 [14].

1.3 Propagation through space and the GZK limit

Hadrons propagating through space interact with CMB photons scattered across the universe. To the hadrons' frame of reference the CMB photons are blue-shifted with

energies of $\sim$ GeV. This implies that photo-meson reactions will take place, where mesons are ejected from the propagating nuclei due to interaction with the high energy gamma rays. In the case of a proton the interaction is mostly

$$p + \gamma_{CMB} \longrightarrow \Delta^{+} \longrightarrow p + k * \pi^{0},\ n + k * \pi^{+}$$

where k is the number of produced pions. Knowing the short decay time of neutrons it is safe to assume the final product will be a proton and a meson. This process limits the energy of the original proton by 20% for each interaction. Greisen, Zatsepin, and Kuzmin concluded that energies above $3 - 4 * 10^{19}$ eV protons won't survive any reasonable astrophysical distance. In figure 1.2 below the GZK horizon of protons has been calculated to be in the order of $\sim$ 100 Mpc.

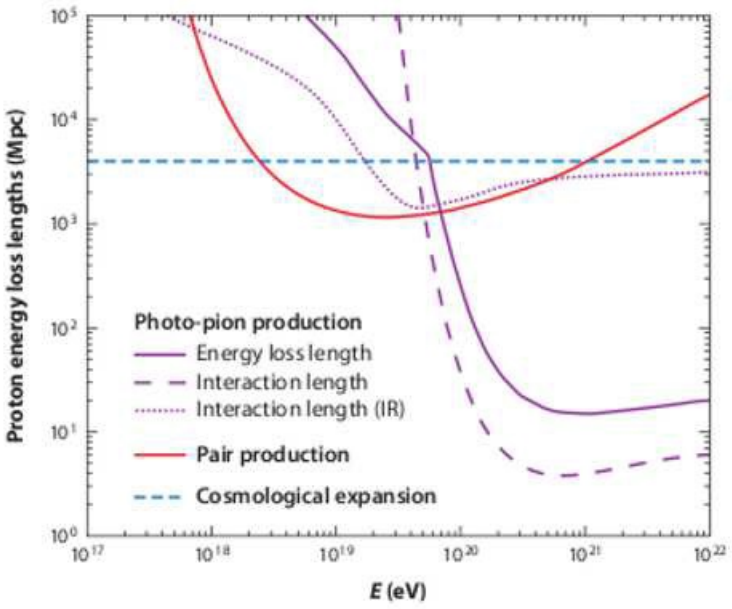

Figure 1.2: Proton energy loss length as function of energy as published by Kotera and Olinto [15].

Other than the GZK effect there has been another theory suggesting an intrinsic loss in the production mechanisms efficiency [16] [17]. From this perspective heavy nuclei cannot be well contained beyond the observed cutoff at $2 - 3 * 10^{19}$ eV.

1.4 Possible sources of UHECR

Covering the possible sources of UHECR is outside the scope of this thesis, yet the reader might find it interesting for further readings, for this reason some of the important candidates could be mentioned here: Active Galactic Nuclei (AGN), Supernova Remnants (SNR), Gamma Ray Bursts (GRB), and neutron stars.

Chapter 2

EAS detection and JEM-EUSO

The concept of EAS and how it is detected will be briefed in this chapter. Moreover in section 2.3 a general overview of the JEM-EUSO experiment will be stated.

2.1 EAS

Extensive air showers occur when UHECR particles interact with nuclei in the atmosphere resulting in a cascade of particles. They have the geometric appearance of an incident particle shower inclined azimuthally to the normal of the earth's surface, and is usually most intense at a specific depth. The depth of the shower through the atmosphere is described by the column density $X[g/cm^2]$, which varies depending on the density of the traversed medium. A generally standard UHECR shower is defined to have $E = 10^{20}eV$, azimuthal angle $\theta = 60^{\circ}$, and X_{max} is where the shower is most intense. The intensity reaches a peak because the energy of each final particle in the shower has reached a critical energy ϵ_0, ceasing further cascades, see figure 2.1 below, and figure 2.2b for an illustration of the X_{max} position:

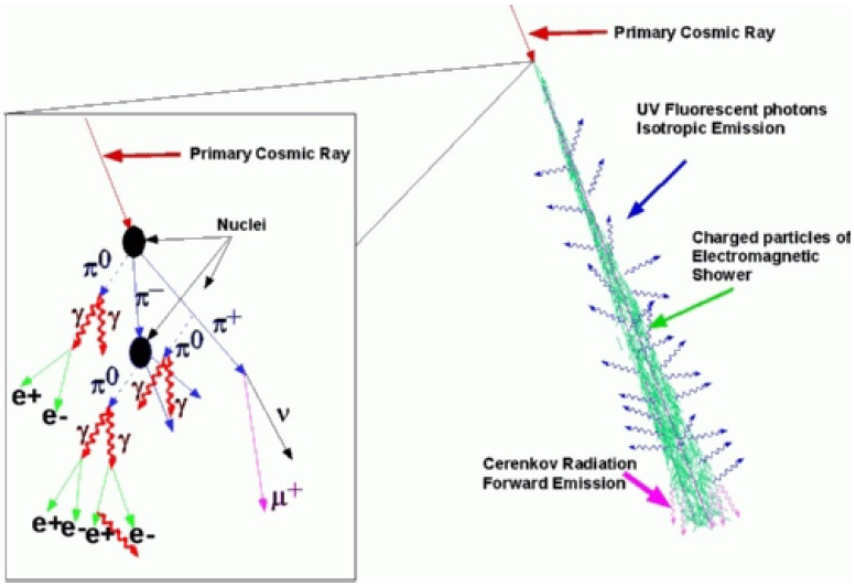

Figure 2.1: Extensive air shower development in the atmosphere. Figure from [22].

2.1.1 Electromagnetic and leptonic showers

In this type of showers an electron or a photon starts an avalanche of particles through the two complementary mechanisms:
- Pair production (PP), where a photon creates an electron-positron pair, and
- Bremsstrahlung, which occur when passing electrons get attracted to atmospheric protons sending out photons with a fraction of its kinetic energy.
Bremsstrahlung has an interaction length of $X_0^{Brem} = 37\ [g/cm^2]$, and PP has $X_0^{PP} = \frac{9}{7}X_0^{Brem}$ [21]. Above the critical energy $\epsilon_0 \sim 10MeV$ brem+PP processes dominate, and below that the only relevant processes are ionization-excitation losses.
X_{max} is proportional to $ln\frac{E}{\epsilon_0}$, which means higher primary energies needs higher number interaction lengths to cool down, see chapter 3. And lastly even though neutrinos have significantly smaller cross section than protons, at the UHE level the cross section becomes considerable. ν:s have the highest X_{max} as they are extremely penetrative particles.

2.1.2 Hadronic showers

Hadronic showers occur in the following manner

$$Hadron + atmospheric\ nuclei \rightarrow hadronic\ shower\ (mostly\ pions)$$

$$\pi^0 \rightarrow 2 * gamma \rightarrow EM\ subshowers$$

$$\pi^{\pm} \rightarrow \mu^{\pm} + \overset{(-)}{\nu}$$

and have the property of higher multiplicity (see the zoomed-in box in figure 2.1), which means that the shower cools off faster and reaches X_{max} earlier than pure EM showers. Also with larger atomic numbers A, the primary energy gets shared to all nucleons of the incoming hadron, giving again lower X_{max} value.

2.2 Detection of EAS

While detecting a specific source of light from the atmosphere one has to consider all the background light effects. They can be categorized as natural and artificial lighting effects. Natural effects include lightning, airglow (UV light created approximately 100 km above sea level by excited O_2 molecules), Earth's albedo (the earth's reflectance ratio which lies around 5% [22]), moon light, aurora, etc.. As for the man-made background light effects there is city light from ground level, planes in the atmospheric level, and satellites from space level.

2.2.1 Fluorescence and Cherenkov

CRs traversing the atmosphere interact with molecules in the air and deposit energy by means of ionization and excitation losses. Excited molecules produce fluorescence light, and the relativistically travelling particles produce Cherenkov light. Gas molecules in air (mainly N_2) get excited by the relativistically propagating charged particles. At the moment of de-excitation, FL is ejected isotropically in the range $\sim 290 - 430nm$.

The Ozone layer however blocks the higher energies of this range, allowing the detection of only $\sim 330 - 430nm$ (O_3 are good UV light absorbers, specifically in the range $\sim 200 - 330nm$). The photon yield has a rising characteristic down to an the altitude of around 11 km above sea level where it's measured to be roughly 4 photons per meter per charged particle, and it declines gradually afterwards [21].

It is known that when a charged particle travels at a speed greater than the speed of light ($v > c$) in medium, Cherenkov light is emitted conically in the same direction of propagation within a narrow angle. CL is detected both directly by the SDs on earth and possibly the reflected amount from earth's surface by detectors in space.

2.2.2 Ground detection

Past and present detectors have been focusing on the detection of FL and CL from ground to reconstruct the shower properties. Some of the most momentous of such detectors are mentioned in the first chapter, but there are other observatories that made some impact with additional statistical knowledge, such as the Telescope Array (TA), Yakutsk, and SuGAr. The most prominent parts from this method are the FDs, SDs, and the underground MDs. Figure 2.2 below shows an illustration of this method:

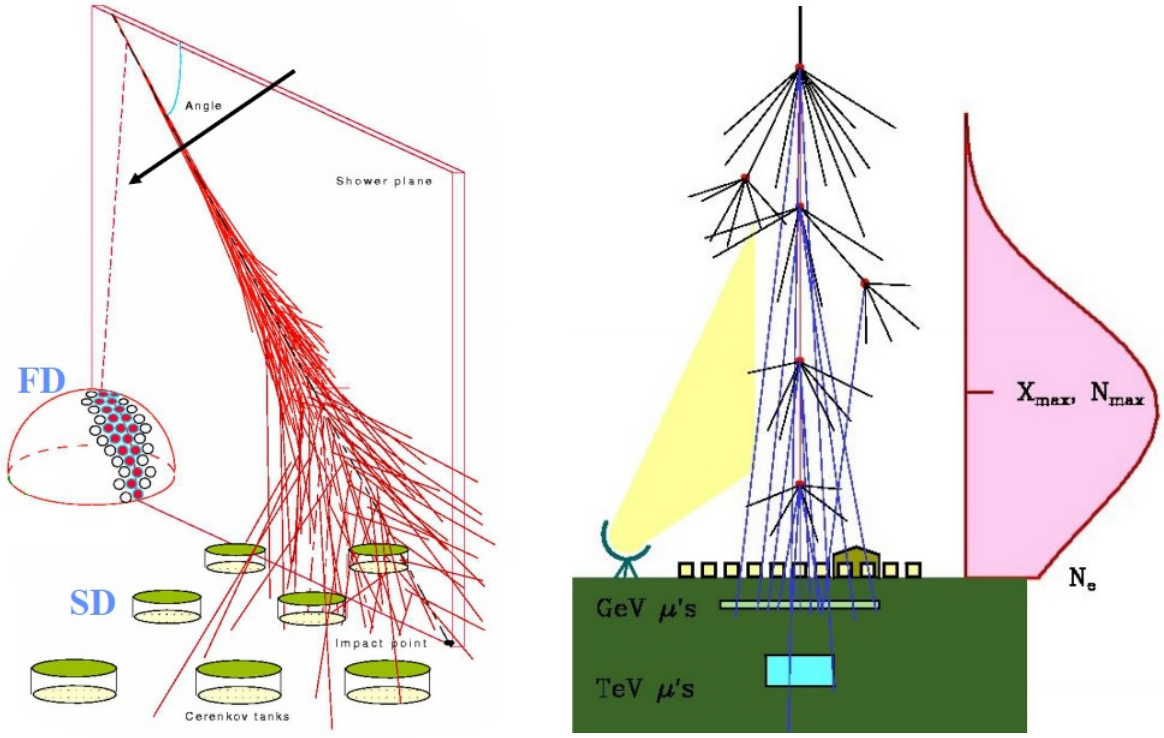

(a) (b)

Figure 2.2: Ground detection methods, utilizing fluorescence detectors as well as surface and underground detectors for Cherenkov and surviving particles from the shower. Figure (a) is taken from [26] and (b) from [18].

2.2.3 Detection from above the atmosphere

Future space detection is currently being developed, and will hopefully provide answers to the main questions swirling around the subject of UHECRs: Are they scattered around the universe isotropically or anisotropically, and what's the composition of CRs as a function of energy? Furthermore a detailed knowledge of the spectrum is needed, which could be acquired with better statistics, with better aperture and wider exposures.

Of the many advantages of space detection, the following are of great value:
- with the current setup planned for JEM-EUSO mission for instance, the exposure rate will be roughly 10 times higher than ground based detection techniques.
- The ability to cover equally both northern and southern hemispheres.
- It will cover much bigger areas.
- Also the aforementioned possibility to detect ground-reflected Cherenkov, which gives additional information on the timing of the shower, thence its geometry.

2.3 JEM-EUSO

The JEM-EUSO experiment has the following requirements to fulfill:
- An observational area $\geqslant 1.3 * 10^5 km^2$, operating for $\geqslant 3\ years$.
- Low enough $E_{threshold}$ for sufficient exposure below $4.4 * 10^{19} eV$.
- Resolutions including: $\theta_{res} \leqslant 2.5^\circ$, $E_{res} \leqslant 30\%$, and $X_{max,res} \leqslant 120 g/cm^2$.

The JEM-EUSO mission is described fully in detail at their official website [27], where they mention the main objectives, exploratory objectives, observational method, and instrumental setup and calibration.

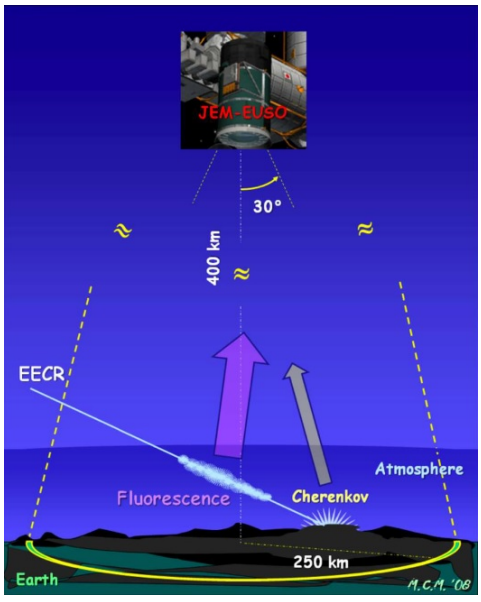

Figure 2.3: An illustration of the exposure to the JEM-EUSO telescope in nadir mode (detector face down on earth, in contrast to tilted mode). Figure taken from [27].

Chapter 3

Analytical Calculations

In this thesis the objective is to make an independent estimate of the amount of photons reaching the detector in space, which should be of the order 10^3. Also how X_{max} for protons vary with different CR energies, and survey the shower size progression throughout the atmosphere.
To tackle the first issue here, we need to think backwards: to know the amount of photons reaching the detector one needs to consider the geometrical aspect of propagation from the shower to the detector in the ISS. Next we need to know how many photons the shower creates and how they are created. Once we know the source that creates photons, what comes to mind is how many creator particles there are in the shower.
As mentioned earlier the incoming primary CR interacts with the atmosphere to create a shower of secondary particles of charged and uncharged nature. The uncharged ones, like the photons proceed into making new EM subshowers by means of pair production until the energy becomes insufficient to interact anymore, where they decay or are absorbed. The charged ones on the other hand may produce Bremsstrahlung photons that create additional subshowers, and fluorescence photons of orders 1-10 eV which penetrate the atmosphere easily and isotropically to be detected on earth or from space.
Based on the GIL function that is derived from the QGSJET model [23], the number of charged particles is:

$$N_{charged} = \frac{E}{1.45\ GeV} e^{f(t)} \tag{3.1}$$

where E is the incoming particle energy, and t is the depth in atmosphere in units of mean interaction length $X_0 = 37 g/cm^2$ after the first interaction (X_1) occured, that is $t = \frac{X - X_1}{X_0}$. The function of $N_{charged}$ reaches its maximum point at t_{max} when $f(t) = 0$, which in turn is defined by:

$$f(t) = t - t_{max} - 2t ln \frac{2}{1 + \frac{t_{max}}{t}} \tag{3.2}$$

and t_{max} as a function of primary energy E and atomic number A being:

$$t_{max} = 1.70 + 0.76 * (ln \frac{E}{81\ MeV} - ln\ A) \tag{3.3}$$

which is essentially based on the theoretical definition of Heitler's toy model of EM cascades [24]. In this model $N_{charged}$ is basically equal to 2^n electrons and photons for n Bremsstrahlung and PP interactions, in other words for $n * X_0$ interactions. With the

energy divided equally, each particle will have the energy $E_n = \frac{E}{2^n}$. At a certain critical energy $E_n = E_c \sim 10\ MeV$ the two mentioned interaction methods will cease to produce further showers, and we obtain the maximum number of charged particles N_{max}:

$$n_{max} = \frac{ln\frac{E}{E_c}}{ln2} = \frac{log_2\frac{E}{E_c}/log_2(e)}{log_2(2)/log_2(e)} = log_2\frac{E}{E_c} \Longrightarrow N_{max} = 2^{n_{max}} = \frac{E}{E_c} \tag{3.4}$$

The parameter 81 MeV in eq. 3.3 is in fact related to E_c, via modifications stemming from the fact that in hadronic showers charged-to-neutral pion ratio is 2:1 (which means a third of the primary energy goes to neutral), and each π^0 decays into 2γ, thus $E \to E/6$ and $E_c = 13.5\ MeV$. X_{max} is then proportional to the logarithm of N_{max}, hence also logarithmically proportional to the primary energy. This behaviour can be seen in figure 4.3.

To better understand the shower development throughout the atmosphere, one needs to relate the amount of created particles to the altitude. For that we need to consider how air pressure vary with altitude. The approach I took here is to define all the necessary parameters in each 10 meter step from above the atmosphere. This way I define an X scale that moves one step each 10 meters. The ingredients of this recipe relies on dimentional analysis and are the following:

$$F = mg, X = m/A \Longrightarrow P = F/A = mg/A = gX,\ \text{so } X = P/g,\ g = GM_\oplus/r^2 \tag{3.5}$$

where F is the gravitational force, A is in area units, P is the air pressure, g is the function for the acceleration of the gravity of Earth, G is the gravitational constant, $M_\oplus$ is the Earth's mass, and r is the Earth's radius in the relevant interval between the Earth's surface and the altitude of the first interaction. The resulting X will then be the column densities at the chosen interval of altitude from the functions of air pressure (see eq. 3.8 and figure 3.1) and Earth's gravity, which then is inserted into the function of $N_{charged}(X)$ to represent the number of charged particles as a function of altitude. Various experiments have been made to determine the photon yield per meter per charged particle from the amount of charged particles, and all agree upon a rising yield down to an altitude of $\sim 11\ km$ and start declining afterwards for all shower ages S (see figure 3.12 in [21]), where age is defined as

$$S = \frac{2}{1 + \frac{t_{max}}{t}} \tag{3.6}$$

For simplicity a 4 photons/m/charged particle yield is assumed throughout the atmosphere [22], and the result is seen in figure 4.2.

Another more usual way of expressing the same thing is to define the altitude as X/ρ, where ρ denotes the air density. This approach will give values for $1X\ [g/cm^2]$ steps instead of a fixed amount of meters, so the end result will give sparse steps at high altitudes and proceed on to much denser steps at the end of the shower at low altitudes. The air density is described by the International Standard Atmosphere equations [25] as follows:

$$\rho = \frac{P * M}{R * T * 1000} \tag{3.7}$$

where the temperature T and the pressure P are described as functions of height H above sea level:

$$T = \begin{cases} T_0 - L * H & \text{if } 0 < H < 11km \\ 217 & \text{if } 11km < H < 20km \\ 197 + H & \text{if } 20 < H < 40km \end{cases} , P = P_0 * (1 - \frac{L * H}{T_0})^{\frac{g*M}{R*L}} \tag{3.8}$$

The constants here are the temperature $T_0 = 288.15\ K$, pressure $P_0 = 101325\ Pa$, and Earth's gravity $g = 9.8\ m/s^2$ at sea level; there are also the temerature lapse rate $L = 6.5\ K/km$, the ideal gas constant $R = 8.31432\ J/(mol \cdot K)$, and the molecular weight of dry air $M = 28.9644\ gm/mol$. The formula of air density is obviously derived from the ideal gas law, which states: $P * V = n * R * T$. Figure 3.2 and 3.3 shows the altitude-temperature and altitude-density relations respectively. Now to relate the column density with altitude, all is needed is to inverse the ρ values to measure from above. This will eventually bring us similar result to that obtained in figure 4.2.

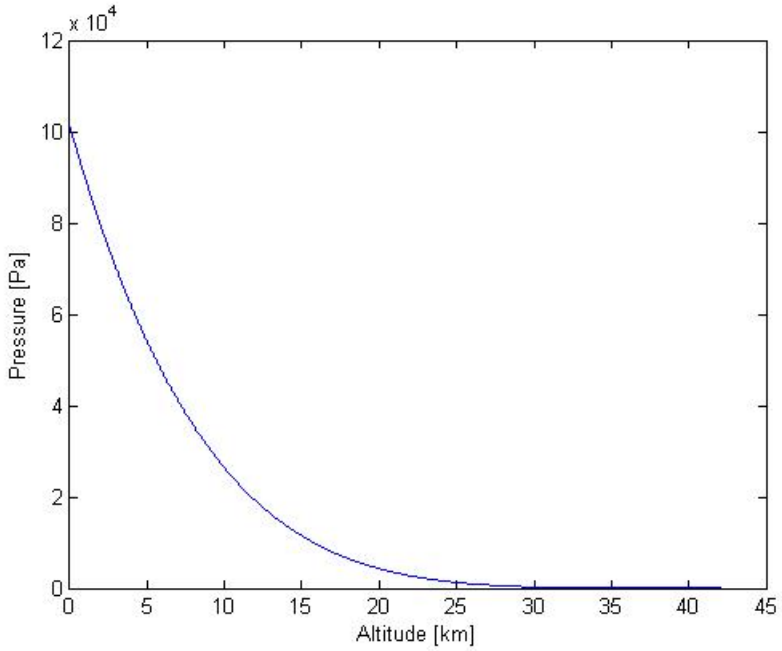

Figure 3.1: Pressure as a function of altitude.

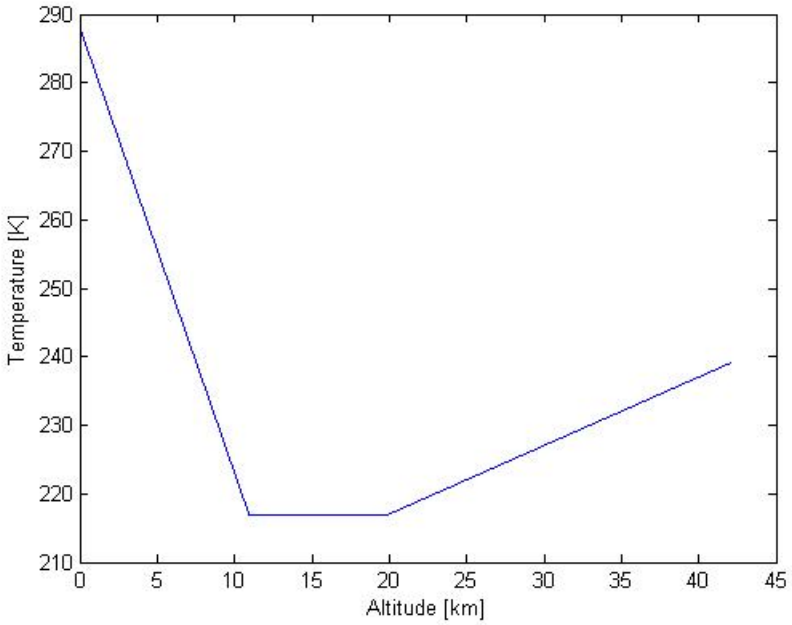

Figure 3.2: Temerature as a function of altitude.

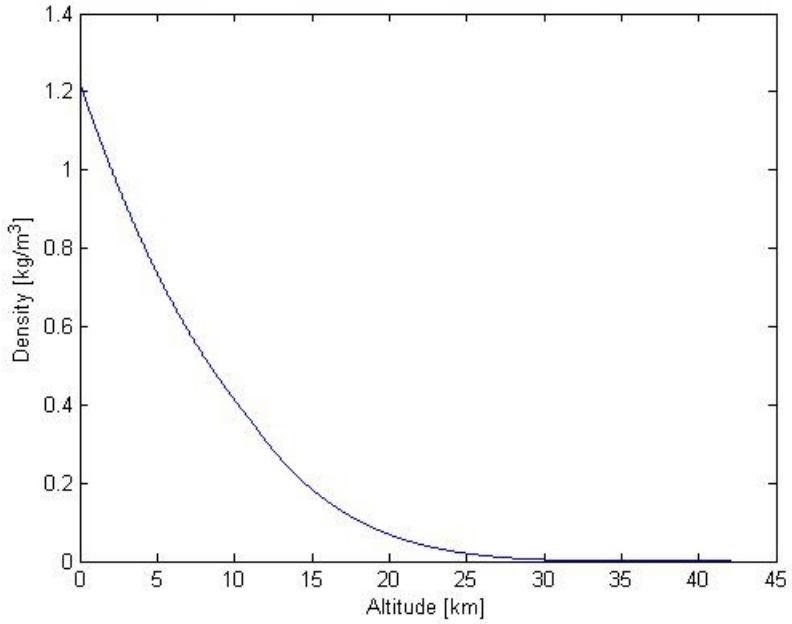

Figure 3.3: Density of air as a function of altitude.

Chapter 4

Results

The number of charged particles has been calculated for all column densities as described in chapter 3, with the equations 3.1 to 3.3. Figure 4.1 shows the amount of charged particles created as a function of depth in the atmosphere. The chosen parameter for the primary energy is $E = 10^{20}\ eV$, $A = 1$ representing protons, and the depth of the first interaction $X_1 = 1\ g/cm^2$.

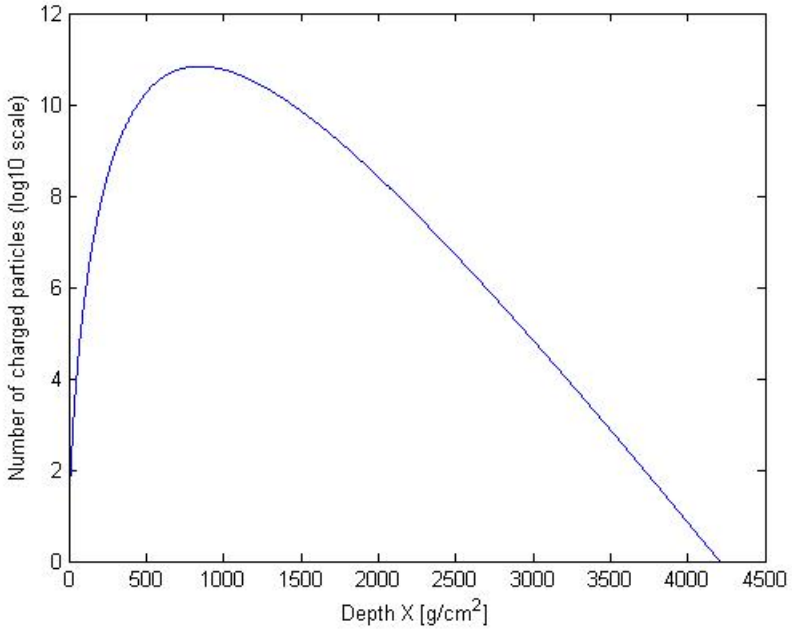

Figure 4.1: The number of charged particles created at various column densities of air for an UHECR proton ($A = 1$) of primary energy $E = 10^{20}$, interacting with the atmosphere at the depth of $X_1 = 1$.

Next step is to find the photon yield, which describes the amount of photons created each meter traversed in the shower. By applying the first method mentioned in chapter 3, figure 4.2 below is obtained, where it is seen to have a maximum yield approximately 25 km after the first interaction in the shower.

The sum of all the photons produced is a direct indicator of the primary CR energy. By integrating over the photon yield throughout the entire atmosphere one gets a total amount of $1.1 * 10^{15}$ photons produced in the shower. Considering now the geometrical

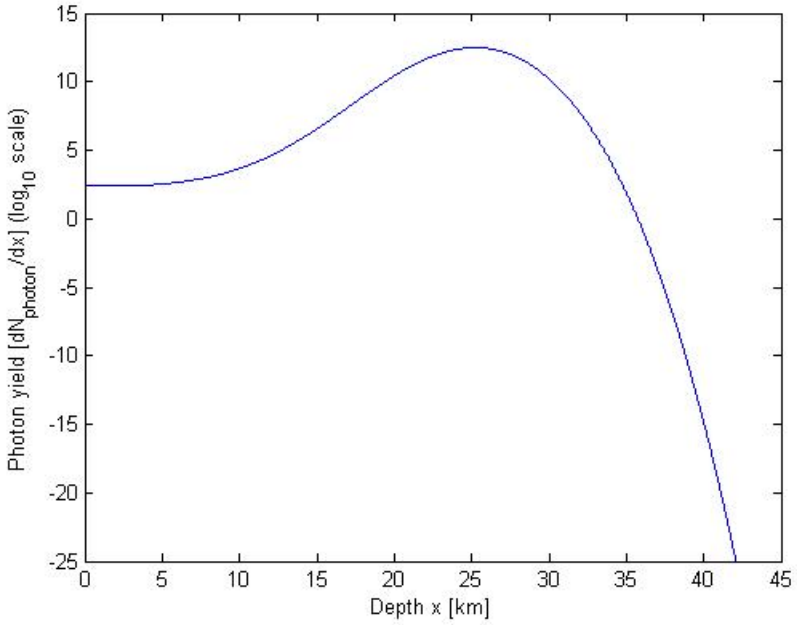

Figure 4.2: The photon yield every 10 meters from above.

aspect of the isotropic propagation to a telescope on the ISS with a double Fresnel lens module with 2.5 m diameter, and assuming a distance of 380 km, a solid angle of $\frac{(1.25)^2\pi}{(\sim 380\ km)^2} sr$ is obtained. The solid angle radius 380 km is an approximative figure for the middle of the shower, which corresponds to a fraction of $\frac{(1.25)^2\pi}{(\sim 380\ km)^2 * 4\pi} \simeq 2.705 * 10^{-12}$. With an azimuthal angle $\theta = 60^\circ$ and an altitude of 40 km for the first interaction in the shower, the distance from the shower to the detector will then vary from 367 km to 400 km. Applying the fraction on the total amount of photons produced, the amount reaching the space detector will then be $\approx 3 * 10^3$.

The total amount of created photons seems to agree with literature [22], which is around 10^{15} photons for an incoming proton of primary energy 10^{20} and azimuthal angle 60 deg. In the simulation of [28] the total amount of fluorescence photons arriving to the detector is 7131, which is around double the amount obtained here, nonetheless it is only stated that several thousands of photons reach the entrance aperture of the telescope in [29]. This may depend on where in the atmosphere the shower starts, and the fact that photon yield is a function of altitude instead of the assumed approximative constant 4 photon/m. Although with the same constant photon yield and a higher start altitude, e.g. 80 km above surface, the amount goes up to around ≈ 4500.

The second part of the thesis work, consists of varying yet another parameter in the charged particle equation 3.1, namely the primary energy. Figure 4.3 is made through tracking the maximum value of the $N_{charged}$ as a function of primary energies in the UHE range above 10^{18} eV.

With a higher atomic number, X_{max} is lower for the same primary energy as discussed earlier in section 2.1.2. This is observed in figure 4.4 below as well as in the upper left plot in figure 1.15 of [21].

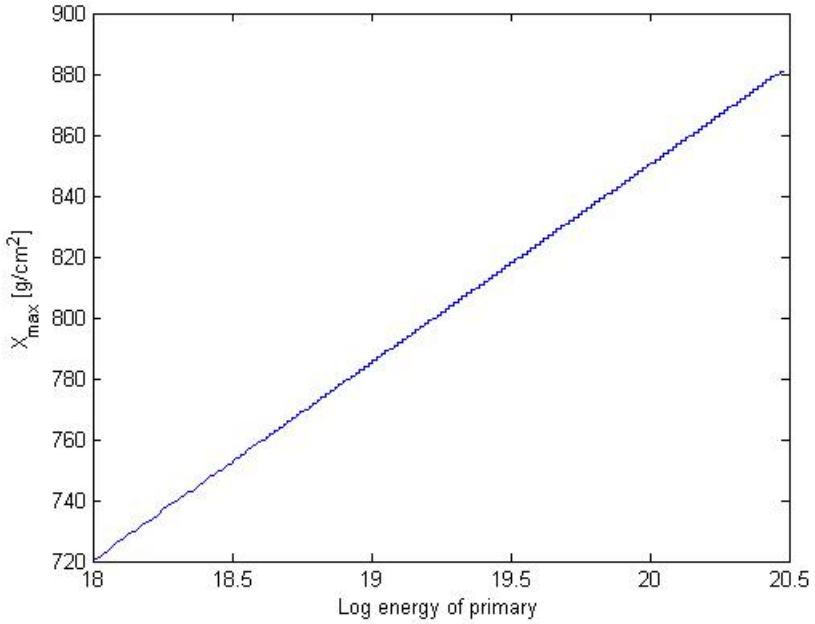

Figure 4.3: X_{max} vs CR Energy.

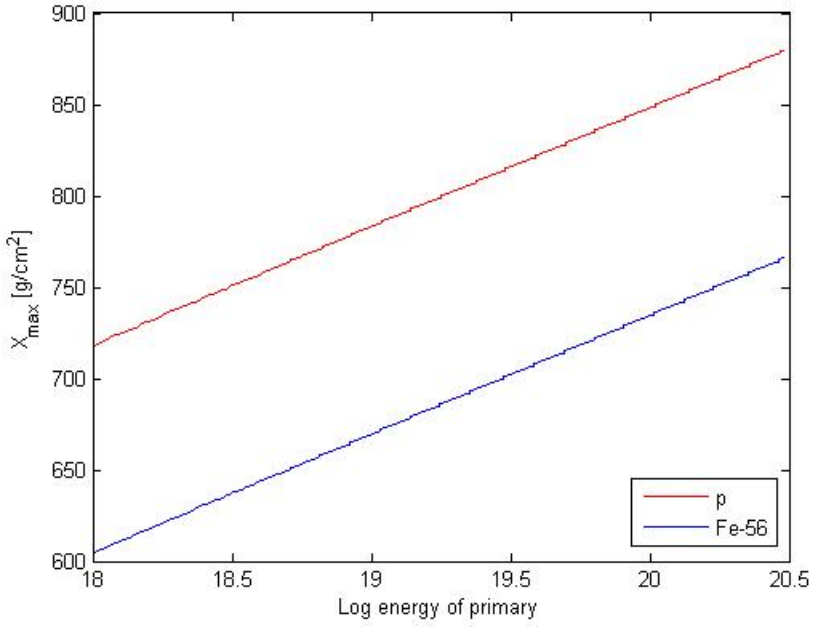

Figure 4.4: The $E - X_{max}$ relation for proton and iron CR.

The percentage of Iron is on the other hand unknown at these UHE ranges. The Primary composition of CRs at energies of order GeV is somewhat: 86% protons, 11% helium nuclei, 2% electrons, and 1% heavier elements [30]. This relation depends on the CR energy, and has almost the same percentages up to around 10^{15} eV. The available low amount of statistics beyond the knee makes composition measurements unfeasible.

Chapter 5

Summary and Conclusions

Collinear motion of showers to primaries means that a space-time fit will provide information about the trajectory of the incoming CR. Tracking these UHECRs will provide clues to the origins of such highly energetic particles.
The size of showers is proportional to the primary energy E of the UHECR, and so is the depth of maximum photon production X_{max} and the type of incoming particles. X_{max} for UHE protons with E at the GZK limit has $X_{max} > 800\ g/cm^2$.

The total amount of photons created in a shower created by an UHECR proton with energy $10^{20}\ eV$ and an inclination angle 60° is $1.1 * 10^{15}$ photons, and the amount of photons that will reach the detector of the JEM-EUSO is roughly $3 * 10^3$ photons.

Bibliography

[1] *The Physics of Cosmic Rays*, a presentation made by the Department of Physics, Purdue University, July 2012.

[2] Seth H. Neddermeyer and Carl. D. Anderson, *Note on the Nature of Cosmic-Ray Particles*, Phys. Rev. **51**, 884 (1937).

[3] H. J. Bhabha, W. Heitler, *The passage of fast electrons and the theory of cosmic showers*, Proc. R. Soc. Lond. Ser. A **159**, 432-458 (1937).

[4] E. Fermi, *On the origin of cosmic radiation*, Phys. Rev. **75**, Nr. 8 (1949).

[5] J. Linsley, L. Scarsi, and B. Rossi, *Extremely Energetic Cosmic-Ray Event*, Phys. Rev. Lett. **6**, 485-487 (1961).

[6] A. Chudakov, *5th Inter-American Seminar on Cosmic Rays*, Bolivia (1962).

[7] K. Greisen, *Proc. Int. Cosmic Ray Conference*, London (1965).

[8] K. Greisen, *End to the cosmic-ray spectrum?*, Phys. Rev. Lett. **16**, 748-750 (1966).

[9] R. Cady, *Progress report on the Utah Fly's Eye*, Int. Cosmic Ray Conference, Bangalore (1983).

[10] `http://www-akeno.icrr.u-tokyo.ac.jp/AGASA/`, *AGASA (Akeno Giant Air Shower Array)*, University of Tokyo, 23-Jul-2013.

[11] Paul Mantsch, *The Pierre Auger Observatory Progress and First Results*, arXiv:astro-ph/0604114, 05-Apr-2006.

[12] R. Benson, J. Linsley, *Satellite observation of cosmic ray air showers*, Int. Cosmic Ray Conference, Paris (1981).

[13] `http://www-spof.gsfc.nasa.gov/Education/wenpart2.html`, *The Exploration of the Earth's Magnetosphere*, Nasa's educational web site, 13-Mar-2006.

[14] S. P. Swordy, *The energy spectra and anisotropies of Cosmic Rays*, Space Science Reviews **99**, 85-94 (2001).

[15] K. Kotera, A. V. Olinto, *The Astrophysics of Ultrahigh-Energy Cosmic Rays*, Ann. Rev. of Astr. and Astroph. **49**, 119-153 (2011).

[16] R. Alosio, *Ultra High Energy Cosmic Rays: The disappointing model*, arXiv:0907.5194v2 [astro-ph.HE] (2011).

[17] R. Alosio et al, *Disappointing model for ultrahigh-energy cosmic rays*, Nucl. Phys. in Astrop. V, Jour. of Phys.: Conf. Series 337 (2012).

[18] Todor Stanev, *Cosmic Rays and Extensive Air Showers Conference*, EDS'09, CERN, July 2009.

[19] Fulvio Melia, *High-Energy Astrophysics*, Princeton, New Jersey: Princeton University Press, 2009.

[20] Todor Stanev, *High Energy Cosmic Rays, 2nd Ed.*, Chichester, UK: Praxis Publishing, 2010.

[21] Francesco Fenu, *A Simulation Study of the JEM-EUSO Mission for the Detection of Ultra–High Energy Cosmic Rays*, 2013.

[22] Thomas Mernik, *JEM-EUSO*, 15-Dec-2009.

[23] D. Naumov, *SLAST, Shower Light Attenuated to the Space Telescope*, EUSO mission internal document, 2003.

[24] W. Heitler, *The Quantum Theory of Radiation (third ed.)*, Oxford University Press, London, p. 386 (Section 38), 1954.

[25] *U.S. Standard Atmosphere, 1976*, National Oceanic and Atmospheric Administration, National Aeronautics and Space Administration, United States Air Force, October 1976.

[26] M. Casolino, *Studing Ultra-High-Energy Cosmic Rays from the International Space Station with JEM-EUSO telescope: status and perspectives*, a presentation made in Stockholm, 2013.

[27] `http://jemeuso.riken.jp/en/index.html`, *JEM-EUSO*, RIKEN, 2013.

[28] M. Bertaina et al., *Performance and air-shower reconstruction techniques for the JEM-EUSO mission*, ScienceDirect **53**, issue 10, 1515-1535, 15-May-2014.

[29] J.H. Adams Jr. et al., *An evaluation of the exposure in nadir observation of the JEM-EUSO mission*, arXiv:1305.2478v1 [astro-ph.HE], 11-May-2013).

[30] M. S. Longair, *High-Energy Astrophysics*, Vol. 1, March 2011.